Journal of Gerontology: BIOLOGICAL SCIENCES
1996, Vol. 51A, No. 4, B295–B302

Accelerated Senile Amyloidosis Induced by Amyloidogenic ApoA-II Gene Shortens the Life Span of Mice But Does Not Accelerate the Rate of Senescence

Keiichi Higuchi,[1] Jing Wang,[1] Kaori Kitagawa,[1]
Takatoshi Matsushita,[1] Kumiko Kogishi,[1] Hironobu Naiki,[2]
Haruo Kitado,[3] and Masanori Hosokawa[1]

[1]Department of Senescence Biology, Chest Disease Research Institute, Kyoto University, Kyoto, Japan.
[2]Department of Pathology, Fukui Medical School, Fukui, Japan.
[3]The Procter and Gamble Company, Japan Technical Center, Kobe, Japan.

The SAMP1 strain is a mouse model for accelerated senescence and severe senile amyloidosis. We studied the effects of the amyloidogenic apolipoprotein A-II gene (Apoa2^c) on senile amyloidosis and the life span and progress of senescence of congenic mice (R1.P1-Apoa2^c) which have Apoa2^c of the SAMP1 strain on the genome of the normally aging SAMR1 strain. Age-associated and severe amyloid deposits were detected in R1.P1-Apoa2^c, as well as a 20% shorter life span than that of SAMR1. The scores of senescence increased more rapidly with age in R1.P1-Apoa2^c than that of SAMR1, and the Gompertz function showed a bigger Y intercept but the same slope of regression line. These results suggest that severe senile amyloidosis induced by the Apoa2^c gene shortens the life span of mice but does not accelerate the rate of senescence.

AGING in higher organisms is a complex process that is probably controlled by a combination of many different factors: genetic, environmental, nutritional, and pathological. Senescence-Accelerated Mouse (SAM) provides a unique model system for the study of the aging process in higher organisms (Takeda et al., 1991, 1994). The SAM strains are murine models of accelerated senescence, which include the senescence-prone SAMP series and the senescence-resistant SAMR series. The SAMP strains grow normally, but then they show early signs of aging: greatly reduced physical activity and loss of hair glossiness, coarseness of the skin, hair loss, periophthalmic lesions, and increased lordokyphosis of the spine. Their life spans are markedly shorter than normal. Analysis of aging dynamics, based on survival curves, scores of senescence, and growth rate, suggests that the aging pattern in the SAMP strains is one of accelerated senescence after normal development (Takeda et al., 1981; Hosokawa et al., 1984). Analysis with the Gompertz function shows that the SAMP strains have the same initial mortality rate (IMR) as the SAMR strains but a shorter mortality rate doubling time (MRDT), presumably due to genes which accelerate the rate of senescence in the SAMP strains (Takeda et al., 1981; Finch, 1990). Molecular genetic characterization of the SAM strains revealed that they might be a group of recombinant inbred strains between the AKR/J strain and an unknown strain developed by some accidental outbreeding (Kitado et al., 1994).

The SAM strains also exhibit a variety of senescence-associated pathologic phenotypes, such as senile amyloidosis (Matsumura et al., 1982; Higuchi et al., 1983), impaired immune responses (Hosokawa et al., 1987), hyperinflation of the lungs (Kurozumi et al., 1994), hearing impairment (Saitoh et al., 1994), degenerative joint disease (Chen et al., 1989), senile osteoporosis (Matsushita et al., 1986), learning and memory deficits (Yagi et al., 1989), and brain atrophy (Shimada et al., 1992, 1994). Among them, senile amyloidosis is one of the most characteristic age-associated disorders in the SAMP strains. All organs, except bone and brain parenchyma, are involved (Takeshita et al., 1982). The severe amyloid deposition throughout the body might be a cause of early death and accelerated senescence in the SAMP strains, but there have been no experimental studies of the role of severe senile amyloidosis in accelerated senescence. ApoA-II, an apolipoprotein in serum high-density lipoprotein (HDL), which is a precursor of murine senile amyloid fibrils (AApoAII), was first isolated from SAMP1 mice (Higuchi et al., 1986a; Yonezu et al., 1986) and was later found to be present universally in mice (Higuchi et al., 1991a; HogenEsch et al., 1993; Shimizu et al., 1993). Three variants of apoA-II protein (types A, B, and C) with different amino acid substitutions at four positions are present among the inbred strains of mice (Higuchi et al., 1991b). The SAMP1, SAMP2, SAMP7, SAMP9, SAMP10, SAMP11, SJL/J, A/J, and LLC strains with a high incidence of senile amyloidosis have type C apoA-II (*Apoa2^c*) with glutamine at position 5, whereas the SAMR1, SAMR4, SAMP6, SAMP8, AKR/J, BALB/c, C57BL/6J, and DDD strains with a low incidence of amyloidosis have type A (*Apoa2^a*) or type B (*Apoa2^b*) apoA-II with proline at position 5. Examination of the genotype of apoA-II gene and

amyloid deposition in the F1, F2, and backcrossed mice made by the crossing of strains with *Apoa2*^{c} and strains with *Apoa2*^{a} or *Apoa2*^{b} showed that early deposition of AApoAII is linked to *Apoa2*^{c} (Higuchi et al., 1991b; Naiki et al., 1993). A congenic strain (R1.P1-*Apoa2*^{c}) of mice which has the amyloidogenic apoA-II gene of SAMP1 (*Apoa2*^{c}) on the genetic background of SAMR1 was developed (Higuchi et al., 1993), and 14-month-old congenic mice showed severe amyloid deposition (Higuchi et al., 1995).

Using the congenic R1.P1-*Apoa2*^{c} and its progenitor SAMR1 strain, whose genomes are different only in a small portion of chromosome 1 surrounding the apoA-II gene, we next studied and report here the effects of accelerated and severe senile amyloidosis caused by the *Apoa2*^{c} gene on life expectancy, the progression of senescence, and pathological findings in mice.

Materials and Methods

Animals. — R1.P1-*Apoa2*^{c} and SAMR1 strains were maintained by sister-brother matings. R1.P1-*Apoa2*$^{b/c}$ mice were produced by crossing SAMR1 mice with R1.P1-*Apoa2*^{c} mice. Mice were reared under conventional conditions at 24 ± 2 °C with a 12-hour light/dark cycle. A commercial diet (CE-2, Nihon CLEA, Tokyo, Japan) and tap water were available ad libitum. At the start of the longitudinal study, 6- to 8-week-old mice of the same gender and strain were selected and housed 5 to 10 in each cage (20 cm wide × 30 cm high × 10 cm deep). Housing groups remained the same with no regrouping throughout their life spans. Fifty female and 50 male R1.P1-*Apoa2*^{c} mice and 19 male and 20 female SAMR1 mice were used for the longevity study. Every 2 months all mice were weighed and their degrees of senescence were evaluated. Mice were inspected at least twice daily, and mice that died spontaneously were necropsied immediately. The liver, spleen, kidney, testis, and heart were weighed, and tissues of the whole body were fixed in 10% neutral buffered formalin, embedded in paraffin, and cut into 4-μm sections that were stained with hematoxylin and eosin or used for histopathologic and immunohistochemical demonstration of amyloid deposition.

Detection of amyloid deposition. — Amyloid was identified by green birefringence in Congo-red stained sections under polarizing microscopy. Amyloid fibril proteins, AApoAII, and amyloid A (AA) protein were immunohistochemically identified by the avidin-biotinylated horseradish peroxidase complex (ABC) method with specific antiserum against AApoAII and murine AA (Higuchi et al., 1983). The amyloid index (AI) was graded 0 to 4 from the degree of AApoAII and AA deposits in the liver, spleen, skin, heart, and stomach in sections stained immunohistochemically with antiserum against mouse AApoAII and AA. Two observers who had no information about the tissue examined, graded AI independently and averaged AI for each mouse.

Mortality rate and life span. — The age at death of each mouse was recorded. To estimate the effect of the genotype of the apoA-II gene on the life span of mice, we determined the maximum life span, mean life span, median survival time (age at 50% survival), and the 10th decile (the mean life span of the last one-tenth of survivors) of the R1.P1-*Apoa2*^{c} and SAMR1 strains. To evaluate the rate of progression of senescence, age-specific mortality rates were calculated for each strain population and analyzed by the Gompertz-Makeham equation (Gompertz, 1825; Finch, 1990). We defined the rate of senescence as the slope of the recognition line in the Gompertz-Makeham equation and calculated the mortality rate doubling time (MRDT) from the slopes for the two strains (Finch, 1990).

Evaluation of degree of senescence. — The degree of senescence was evaluated by our grading system (Hosokawa et al., 1984). Eleven categories of behavioral activity and gross appearances are considered to be associated with the aging process: reactivity, passivity, loss of hair and of glossiness, skin coarseness, skin ulcers, periophthalmic lesions, cataracts, corneal ulcers, corneal opacity, and lordokyphosis of the spine. Each category is graded 0 to 4 according to the degree of change, and the grading score for each mouse is the sum of the grades of each category. Since grading scores increased irreversibly and universally with advancing age in all the strains of mice tested and there was a statistically significant reverse correlation between the remaining life span and the total scores of grading, this grading score appears valid for evaluation of the degree of senescence (Hosokawa et al., 1984; Hosokawa, 1994). Generally, the grading was done at a fixed time from 2 p.m. to 4 p.m. by two independent observers who were not told the strain or the age of the mice examined.

Statistical analysis. — All data are presented as the mean ± *SEM*. A Statistical Analysis System (SAS) package (SAS Institute, Tokyo) was used to analyze the data. Three-way analysis of variance (ANOVA) of strain, sex, and age (repeated measures) was used to compare body weights of the mice with the two genotypes of apoA-II gene at various ages. Survival curves were estimated by the Kaplan-Meier test (Kaplan and Meier, 1958), and they were compared with the Wilcoxon test (Steel and Torrie, 1980). The grading scores of senescence and the AI of AApoAII deposition in the two strains (R1.P1-*Apoa2*^{c} and SAMR1) were compared with the Mann-Whitney's test (Steel and Torrie, 1980). The incidence of each pathological finding in the two strains was compared with the Fisher's exact test (Steel and Torrie, 1980). The AI and age were correlated with Spearman's rank test (Steel and Torrie, 1980). The comparison of regression lines correlating age-specific mortality rate with age, and AI with age, was determined by the analysis of covariance with the SAS system. The mean life span and 10th decile in the two strains were compared with the Student's *t*-test.

Results

Growth curve and longevity. — Both strains (R1.P1-*Apoa2*^{c} and SAMR1) showed similar age-related changes in body weight from 100 to 500 days of age (Figure 1). Three-way ANOVA of strain, sex, and age (repeated measures between 100 and 500 days) showed that sex and age effects were significant ($p < .01$), but strain effect was not signifi-

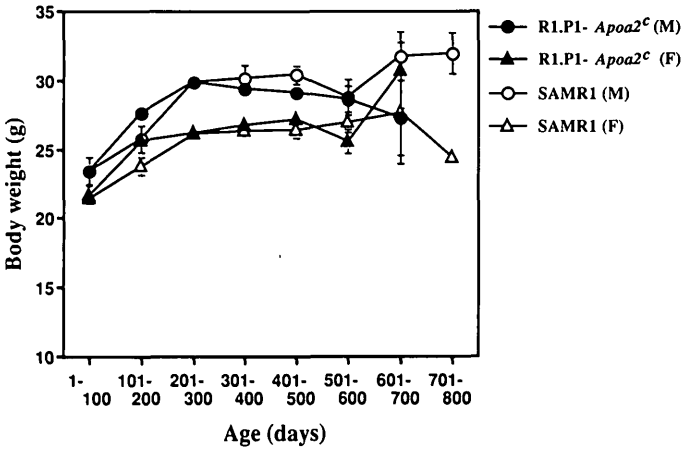

Figure 1. Age-related changes in body weight of apoA-II congenic strains of mice. Each point is the mean ± *SEM* of mice in each age group. Nineteen male and 20 female SAMR1 mice and 50 male and 50 female R1.P1-*Apoa2*^{c} mice aged 6–8 weeks were used. M = male, F = female. Three-way ANOVA of strain, sex, and age (repeated measures between 100 and 500 days) showed that sex and age effects were significant ($p < .01$) but strain effect was not significant. The male mice weighed significantly more than the female mice of both strains after 200–500 days of age ($p < .01$, Newman-Keuls procedure).

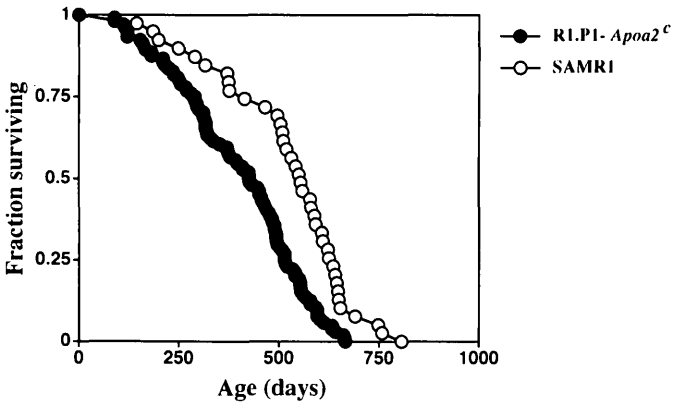

Figure 2. Survival curves of apoA-II congenic strains of mice. The number of mice of each strain used is as noted for Figure 1. Since there was no significant sex difference in either strain, fraction surviving was calculated from the combined data for both sexes in each strain. The survival curves of the two strains differed significantly ($p < .01$, Wilcoxon test).

Table 1. Parameters of Life Span in ApoA-II Congenic Strains

	Strain	
	R1.P1-*Apoa2*^{c}	SAMR1
Number of mice	100	39
Maximum life span (days)	666	807
Age at 50% survival (days)	426	555
Mean life span (days)	400.92 ± 15.16[a]	521.26 ± 25.64
10th decile (days)[c]	630.60 ± 27.76[b] (10)	731.20 ± 48.01 (4)

Note. Values of mean life span and 10th decile represent the mean ± *SEM*.

[a]The mean life span in R1.P1-*Apoa2*^{c} was significantly shorter than that of SAMR1 ($p < .01$, Student's *t*-test).

[b]The 10th decile in R1.P1-*Apoa2*^{c} was significantly shorter than that of SAMR1 ($p < .01$, Student's *t*-test).

[c]Mean life span of last one-tenth of each group to survive was calculated. The numbers in parentheses are the numbers of surviving mice.

cant. The body weights of male mice were significantly higher than those of female mice of both strains after 200–500 days of age ($p < .01$, Newman-Keuls procedure). The strain and age interaction was significant ($p < .05$), and the Newman-Keuls procedure revealed that R1.P1-*Apoa2*^{c} weighed significantly more than SAMR1 only at 101–200 days of age ($p < .05$). After the age of 600 days, the range of body weight increased in both strains. The survival curve of the R1.P1-*Apoa2*^{c} strain shifted to the left (to a younger age) from the curve of the progenitor SAMR1 strain (Figure 2). The survival curves of the two strains differed significantly ($p < .01$, Wilcoxon test). There was no significant gender difference within each strain (data not shown). Four parameters of life span were determined for the two strains (Table 1). Maximum life span (666 days) and the age at 50% survival (426 days) in the R1.P1-*Apoa2*^{c} strain were 18% and 24% shorter, respectively, than in the progenitor SAMR1 strain (807 and 555 days) when the *Apoa2*^{b} gene was replaced with the *Apoa2*^{c} gene in the SAMR1 strain. The mean life span of R1.P1-*Apoa2*^{c} strain was significantly (24%) shorter than that of the SAMR1 strain ($p < .01$, Student's *t*-test). There was no significant gender difference in mean life span within each strain (R1.P1-*Apoa2*^{c} males 432.00 ± 22.63 days; females 387.36 ± 22.78 days, $p > 0.1$; and SAMR1 males 529.53 ± 41.41 days; females 513.40 ± 33.40 days, $p > 0.1$). The 10th decile, which is the mean life span of the last one-tenth of each group to survive, in the R1.P1-*Apoa2*^{c} strain was 14% shorter than in the SAMR1 strain ($p < .01$, Student's *t*-test).

Simple linear regression of age-specific mortality rates (after $\log_{10}$ transformation) in relation to chronological age was used to analyze the effect of *Apoa2*^{c} on the rate of senescence (Figure 3). In each apoA-II congenic strain, linear regression was obvious and significant, so we applied a simple working model of the Gompertz equation: $m(t) = A10^{\alpha t}$, where $m(t)$ is the age-specific mortality rate and α is the rate constant for age-related increase of mortality, corresponding to the slope of regression line. There was no significant difference in the slopes of the regression lines of the two strains (α = .0025 in the R1.P1-*Apoa2*^{c} strain and α = .0024 in the SAMR1 strain). The mortality rate doubling time (MRDT) calculated for each strain in reference to α was almost the same (.330 year in the R1.P1-*Apoa2*^{c} strain and .344 year in the SAMR1 strain). In contrast, the initial mortality rate (IMR), which was calculated as an intercept of $t = 0$, was significantly different: .157/year in the R1.P1-*Apoa2*^{c} strain and .073/year in the SAMR1 strain ($p < .01$).

Grading scores of senescence. — Grading scores of senescence increased with aging in the apoA-II congenic strains (Figure 4). There was no significant gender difference in scores in each strain except for the higher score in male than in female R1.P1-*Apoa2*^{c} mice aged 501–600 days and the lower score in male SAMR1 mice aged 201–300 days ($p < .05$, Mann-Whitney's test; data not shown). Therefore, we combined the scores for both sexes in each strain in Figure 4. Throughout life, all age groups of R1.P1-*Apoa2*^{c} mice

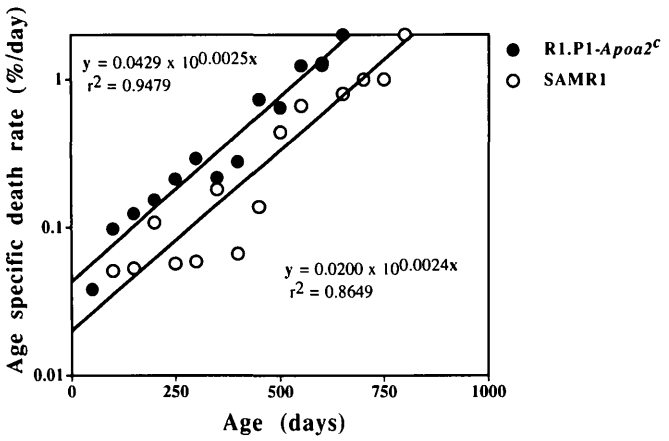

Figure 3. Gompertz functions for apoA-II congenic strains. Mortality rates were calculated for each 50-day period throughout the life of the R1.P1-*Apoa2*^{c} and SAMR1 strains and plotted as a function of age. Lines are plotted on the basis of the least-squares regression for estimation of the initial mortality rate (A), mortality rate at day 0, and exponential Gompertz component (α), which describes the age-related rate of acceleration of the mortality rate. The comparison of the two regression parameters and intercepts revealed that the initial mortality rate for the R1.P1-*Apoa2*^{c} strain was significantly higher ($p < .01$) than that of the SAMR1 strain, whereas there was no significant difference in the exponential Gompertz component.

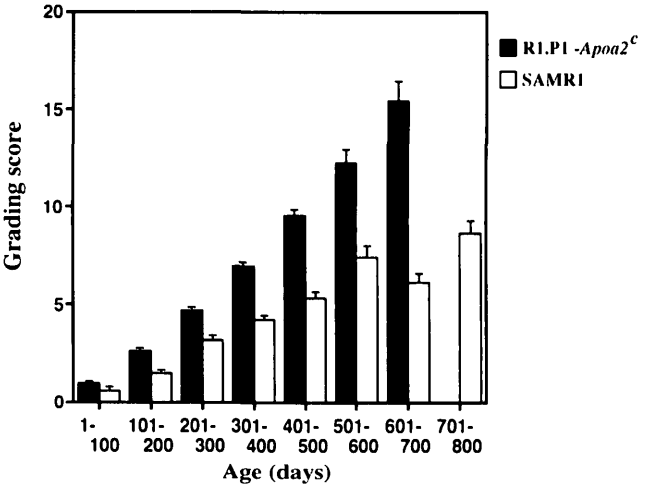

Figure 4. Age-related changes of grading scores in apoA-II congenic strains of mice. The degree of senescence of each mouse was recorded by the grading scores of senescence (Hosokawa et al., 1984) for each 100-day period throughout the life of the R1.P1-*Apoa2*^{c} and SAMR1 strains. The values are means ± *SEM* of mice in each age group. Grading scores were calculated from the combined data for both sexes of each strain. There was a significant difference in the scores between the two strains throughout life except during the first 100 days ($p < .01$ by Mann-Whitney's test).

showed significantly higher scores of senescence than did SAMR1 mice ($p < .01$) except during the first 100 days. Finally, the score reached 15 in R1.P1-*Apoa2*^{c} mice and 8 in SAMR1 mice. Eleven items were included in the grading system. In the R1.P1-*Apoa2*^{c} strain, a characteristic increase in any specific item was noted, but almost all items had higher scores than those in SAMR1 mice (data not shown).

Genotype of apoA-II gene and amyloid deposition. — Fifty-eight R1.P1-*Apoa2*^{c} mice (28 males and 30 females) and 26 SAMR1 mice (15 males and 11 females) without severe autolysis were selected for pathological examination. AApoAII and AA amyloid deposition in the tissues was demonstrated by an immunohistochemical technique with anti-apoA-II and anti-AA antisera. Amyloid deposition in 19 R1.P1-*Apoa2*$^{b/c}$ mice (13 males and 6 females) which had died naturally was examined to evaluate the dosage effect of *Apoa2*^{c} gene on amyloid deposition. The amyloid index (AI), which represents semiquantitatively the intensity of AApoAII deposition in the tissues, was calculated for each strain (Figure 5). In the R1.P1-*Apoa2*^{c} strain, AApoAII deposition was first observed in the spleen, liver, skin, and small intestine of a mouse which died at 250 days of age, and all mice older than that had AApoAII deposition. The intensity of AApoAII deposition increased linearly with age ($p < .01$, Spearman's rank test), and AApoAII deposits were present throughout the whole body of old R1.P1-*Apoa2*^{c} mice. In clear contrast, the only SAMR1 mouse with AApoAII deposition was a 753-day-old mouse which had slight AApoAII deposition in the skin. In R1.P1-*Apoa2*$^{b/c}$ mice, which are heterozygous for type B and type C apoA-II, the onset of AApoAII deposition was significantly later than in the homozygous R1.P1-*Apoa2*^{c} strain. The AI increased more slowly with advancing age in R1.P1-*Apoa2*$^{b/c}$

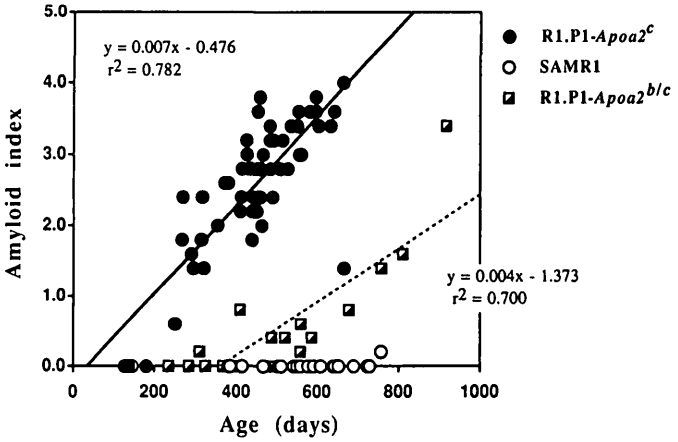

Figure 5. AApoAII deposition in apoA-II congenic strains of mice. The AI was calculated in immuno-stained tissues as an indicator of the intensity of AApoAII deposition. Linear regression and correlation were calculated. There were significant correlations between AI and age in R1.P1-*Apoa2*^{c} and R1.P1-*Apo*$^{b/c}$ mice with Spearman's rank test ($p < .01$). The effect of the *Apoa2*^{c} gene dosage on amyloid deposition (AI) was significant with covariant analysis ($p < .01$). There was no significant sex difference for AI within each group (Mann-Whitney's test).

than in R1.P1-*Apoa2*^{c} mice. There was no significant sex difference in the AI in either strain (Mann-Whitney's test).

AA amyloid deposition was detected in spleen, skin, heart, thyroid, intestine, kidney, and stomach of 15 R1.P1-*Apoa2*^{c} mice, 2 SAMR1 mice, and 6 R1.P1-*Apoa2*$^{b/c}$ mice, and the AI of each mouse was calculated (Figure 6). Autopsy revealed various inflammatory lesions: skin ulcer (9 mice); abscesses in the liver, kidney, skin, heart, and tail (8 mice); and pneumonia (6 mice) in mice which had AA deposition. In contrast to AApoAII, there was no correlation between

the AI for AA and age in R1.P1-*Apoa2*^{c} or R1.P1-*Apoa2*$^{b/c}$ mice (Spearman's rank test).

Other pathological findings. — The primary pathological findings were inflammatory changes (mainly pneumonia and abscess), tumors (mainly malignant lymphoma), amyloidosis (AApoAII or AA deposition), and contracted kidney (Table 2). The incidence of pneumonia and other inflammations (skin ulcer; abscesses in the liver, lung, skin, heart, kidney, and brain) was not significantly different in the two apoA-II congenic strains. The incidence of malignant nonthymic lymphoma was significantly lower in the R1.P1-*Apoa2*^{c} than in the SAMR1 strain ($p < .01$, Fisher's exact test). Other tumors were histiocytic neoplasm in two SAMR1 mice and two R1.P1-*Apoa2*^{c} mice and granulocytic neoplasm in one SAMR1 mouse. The three R1.P1-*Apoa2*^{c} mice which died before 180 days of age were the only ones with no AApoAII deposition. In contrast, only the oldest SAMR1 mouse, which died at 758 days of age, had AApoAII depositions. The incidence of AA deposition tended to be higher ($p < .075$, Fisher's exact test) in the R1.P1-*Apoa2*^{c} strain than noted in the SAMR1 strain. Depositions of both AApoAII and AA were noted in 13 R1.P1-*Apoa2*^{c} mice and one SAMR1 mouse. The incidence of contracted kidney was significantly higher in the R1.P1-*Apoa2*^{c} strain than in the SAMR1 strain. Severe AApoAII depositions were observed in the kidneys of all R1.P1-*Apoa2*^{c} mice with contracted kidney. AApoAII deposits were mainly in the papillae and parenchymal tissues of the kidney, but rarely in the glomerulus. In the six R1.P1-*Apoa2*^{c} mice with contracted kidney, AA deposits were mainly in the glomerulus. In the SAMR1 mouse with contracted kidney, severe AA deposition was present in the glomerulus, parenchymal tissues, and papillae of the kidney, perhaps secondary to the abscess found in the kidney. In this mouse, severe AA depositions were also present in all the other organs.

Other pathological findings which might have caused death were massive bleeding in an ovarian cyst (four R1.P1-*Apoa2*^{c} mice and two SAMR1 mice) and invagination of the intestine (two R1.P1-*Apoa2*^{c} mice). We could detect no pathological findings in one R1.P1-*Apoa2*^{c} mouse (181 days old) and three SAMR1 mice (384, 511, and 550 days old).

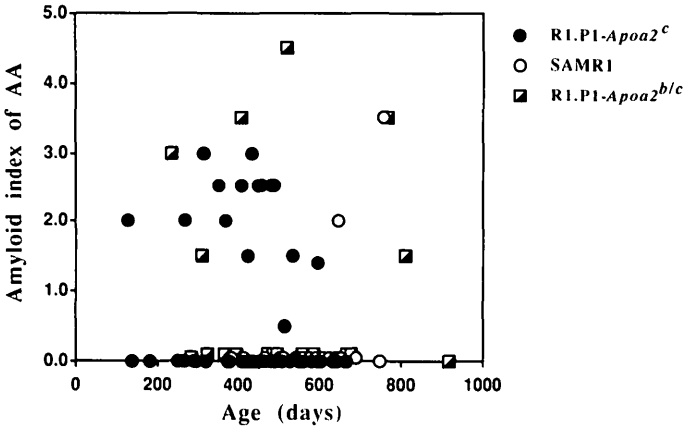

Figure 6. AA deposition in apoA-II congenic strains of mice. The AI was calculated in immuno-stained tissues as an indicator of the intensity of AA deposition. AI for AA did not show any sex difference in either strains (Mann-Whitney's test). There was no significant correlation between AI for AA and age in either strain with Spearman's rank test.

DISCUSSION

The Gompertz mortality model has been used to describe senescence of populations. Two mortality rate parameters limit life span, the mortality rate doubling time (MRDT), and the initial mortality rate (IMR). The age-related acceleration of the mortality rate is measured as the MRDT, which is considered to be a fundamental measure of the rate of senescence. MRDT of different inbred strains is overall stable and statistically indistinguishable, even for the NZB and SJL/J strains that die prematurely, from lymphoreticular sarcomas (Storer, 1978; Finch, 1990). SAMP strain mice, models of accelerated senescence, have significantly shorter life spans and shorter MRDTs than do SAMR strain mice, which have normal senescence and were used as controls (Takeda et al., 1981, 1994). This accelerated senescence may also occur at the level of cultured fibroblast-like cells (Hosokawa et al., 1994).

What are the genetic factors responsible for the accelerated senescence of the SAMP strains? In this report we determined the effect of a candidate gene, *Apoa2*^{c}, on the life span and rate of senescence. We chose the *Apoa2*^{c} gene for the following reasons: (1) severe senile (AApoAII) amyloidosis, in which apoA-II protein is deposited as amyloid fibrils, is the most characteristic pathological finding in SAMP strains, and we

Table 2. Pathological Findings in the ApoA-II Congenic Strains

Strains	n[a]	Pathological Findings						
		Pneumonia	Other Inflammations	Lymphoma	Other Tumors	Amyloidosis		Contracted Kidneys
						AApoAII	AA	
R1.P1-*Apoa2*^{c}	58	25 (43.1)[b]	18 (22.3)	1* (1.7)	2 (3.4)	55* (94.8)	15 (25.9)	27* (46.5)
SAMR1	23	8 (34.8)	4 (17.4)	6 (26.1)	3 (13.0)	1 (4.3)	2 (8.7)	1 (4.3)

[a]Animals with advanced postmortem changes were excluded.

[b]The numbers in parentheses give the percentage of the mice with pathological findings in each strain.

*Significant difference from the SAMR1 strain ($p < .01$, Fisher's exact test).

have shown that the *Apoa2*^{c} gene carried by many SAMP strains may induce severe amyloidosis (Higuchi et al., 1991a, 1991b, 1995; Naiki et al., 1993); (2) amyloid fibril deposits of various origins from different proteins are found at an advanced age in many animal species and are considered to be among the pathological criteria of aging and of the progeroid syndrome in humans (Martin et al., 1978; Higuchi and Takeda, 1986b); (3) F2 and backcrossed mice with the homozygous *Apoa2*^{c} allele have significantly higher grading scores of senescence than do mice with the homozygous *Apoa2*^{b} allele or heterozygous alleles for *Apoa2*^{b} and *Apoa2*^{c} in the experiment of genetic crossing between SAMP1 and SAMR1 (Naiki et al., 1993); and (4) one locus linked to mouse longevity is placed close to the *Apoa2* gene (Gelman et al., 1988), and the *Mpmv-29* locus close to *Apoa2* is present in several SAMP strains but no SAMR strains (Kitado et al., 1994). The congenic strain, derived from SAMR1 which carries a very small chromosomal region surrounding the *Apoa2*^{c} gene of SAMP1 (R1.P1-*Apoa2*^{c}), should be the best tool for evaluating the effect of the *Apoa2*^{c} gene. *Apoa2*^{c} causes severe AApoAII amyloidosis and shortens the life span of R1.P1-*Apoa2*^{c} mice but does not change the MRDT. Thus, *Apoa2*^{c} shortens the life span by increasing the IMR in the congenic strain. Our results indicate clearly that there are other genetic factors responsible for accelerated senescence and shortening the MRDT in SAMP strains.

The onset of amyloidosis, characterized by the extracellular accumulation of fine amyloid fibrils, is usually in the middle and late stages of life (Cohen and Jones, 1993). Amyloid deposition is reported to induce various degenerative changes in the tissues (Lorenzo et al., 1994; Maury, 1995) of patients with several types of amyloidosis and to shorten their lives. In mice, however, no particular degenerative effects of AApoAII have been described (Higuchi et al., 1984), and the relatively slight shortening (about 20%) of life span of R1.P1-*Apoa2*^{c} might suggest that AApoAII causes only slight damage to the tissues. However, severe AApoAII deposition replaces and destroys cells throughout the body and might accelerate the age-related functional loss of each tissue. This accelerated functional loss might increase the grading scores of senescence in the congenic strain and increase the IMR. It is especially true that AApoAII deposition in the papillae and parenchymal tissue of the kidney may cause contracted kidney and shorten the life span of mice (Table 2).

The grading score system was developed in our laboratory for evaluation of the degree of senescence of mice and maintenance of the phenotype of accelerated senescence in SAMP strains. This system was designed to satisfy the following criteria: (1) appropriate for longitudinal studies of individual mice, (2) easy to apply, (3) results expressed numerically and analyzed statistically, and (4) objective and reproducible grading scores (Hosokawa, 1994). Mice are graded according to clearly defined criteria (Takeda et al., 1981). This system has also been used as a method to evaluate the effect of manipulations which modify life span and senescence in our and other laboratories (Kohno et al., 1985; Zhao and Nomura, 1990; Umezawa et al., 1993; Naiki et al., 1993). The grading system consists of 11 items which are classified into four groups: behavioral, gross appearance of the skin, ophthalmic lesions, and lordokyphosis of the spine. Higher scores in all groups in the R1.P1-*Apoa2*^{c} strain suggest that the *Apoa2*^{c} gene might hasten general senescence. In the R1.P1-*Apoa2*^{c} strain, the age-related decrease of serum levels of HDL is accelerated (Higuchi et al., 1995). Analysis of other age-related changes, such as chromosomal aberrations (Nisitani et al., 1990) and impaired immune responsiveness (Hosokawa et al., 1987) in the R1.P1-*Apoa2*^{c} strain, will help us to evaluate general effect of the *Apoa2*^{c} gene on senescence acceleration. Model mouse strains for common age-related disorders such as atherosclerosis (Paigen et al., 1987; Zang et al., 1992; Warden et al., 1993), autoimmune reactions (Gardner et al., 1977; Hang et al., 1982), diabetes (Coleman, 1978; Makino et al., 1980), and obesity (Lane and Dickie, 1958) should have shorter life spans. However, there have been few population analyses of the effects on the rate of senescence of the genes responsible for the early onset of these age-related disorders. We developed apoA-II congenic strains and showed that the *Apoa2*^{c} gene induces the early onset of severe senile amyloidosis which shortens the life span and hastens senescence in mice. Studies of these congenic or transgenic strains of mice are essential for the precise evaluation of the effect of the genotypes of genes without interferences by numerous and unidentifiable genes in the late stage of life.

The aging dynamics of an inbred strain of mice might vary with conditions of rearing. The age at 50% survival (555 days) and the grading score (3.23 at 201–300 days of age) of the SAMR1 strain in this study were almost the same as the data (568 days and 3.36 at 8 months of age) which were most recently determined for SAMR1 in our laboratory (Takeda et al., 1994). The two strains examined here were housed under conventional conditions. Although serological tests were negative for major pathogens such as HVJ (hemagglutinating virus of Japan), MHV (mouse hepatitis virus), *Salmonella typhimutium*, *Bacillus piliformis*, etc., the relatively high incidence of pneumonia and other inflammations in both strains (Table 2) suggests the possibility that environmental pathogens might have influenced the aging dynamics of the two strains. Studies in improved environmental conditions such as specific pathogen-free (SPF) housing should be done to determine precisely the effects of environment on the aging process and amyloid deposition.

The onset of AApoAII senile amyloidosis in R1.P1-*Apoa2*^{c} mice occurs much earlier and the severity of amyloid deposition is far greater than in heterozygous R1.P1-*Apoa2*$^{b/c}$ mice (Figure 5). The gene dosage effect of *Apoa2*^{c} was also suggested in our previous genetic cross studies (Higuchi et al., 1991b; Naiki et al., 1993). Most types of inherited amyloidosis in humans are transmitted in the autosomal dominant form (Benson, 1991). Development of amyloid fibril deposition and manifestations of the clinical syndrome are associated with mutant forms of fibril precursor proteins: transthyretin in familial amyloid polyneuropathy (FAP) type I, apolipoprotein A-I in familial amyloid polyneuropathy Iowa type, gelsolin in Finnish hereditary amyloidosis, cystatin C in the hereditary cerebral hemorrhage with amyloidosis in Iceland, ß amyloid precursor protein in Dutch-type hereditary cerebral hemorrhage with amyloidosis and Swedish familial Alzheimer's disease, and lysozyme in hereditary

non-neuropathic systemic amyloidosis (Cohen and Jones, 1993; Maury, 1995). Several homozygous patients have been found in some FAP families; however, most patients with hereditary amyloidosis are heterozygous. No gene dosage effect on the severity of symptoms has been found in those families (Holmgren et al., 1988; Yoshinaga et al., 1992). We have no clear explanation for the *Apoa2*^{c} dosage effect in mice. Kinetic analysis of AApoAII amyloid fibril formation in vitro indicates that the rate of fibril elongation is proportional to the concentration of Apoa2^c protein in the reaction (Naiki et al., 1991). However, the serum apoA-II concentration is much lower in the *Apoa2*^{c} strain than in the *Apoa2*^{b} strain and decreases markedly with age (Kitagawa et al., 1994; Higuchi et al., 1995). *Apoa2*^{c} gene dosage effects were obvious in the size of HDL particles in which almost all of the apoA-II protein circulates together with other apolipoproteins and lipids (Higuchi et al., 1993; Ishikawa et al., 1994), but *Apoa2*^{a} strains (e.g., C57BL/6J) also have small HDL particles like *Apoa2*^{c} strains (Mehrabian et al., 1992). To understand the mechanisms of amyloidogenesis and the dosage effect of *Apoa2*^{c}, we need to know the precise characteristics of the Apoa2^c protein when it interacts with Apoa2^c itself or Apoa2^b protein, and with pathological molecular chaperones such as apoE during fibrilization. The deposition of AA protein in secondary amyloidosis is induced by inflammatory reaction. The incidence of inflammation in the R1.P1-*Apoa2*^{c} strain and the SAMR1 strain was almost the same, but the incidence of AA amyloid deposition was higher in the R1.P1-*Apoa2*^{c} strain than in the SAMR1 strain (Table 2). Two hypotheses may explain this finding: (1) a gene located very close to the *Apoa2*^{c} gene may regulate susceptibility to secondary amyloidosis, or (2) microenvironmental changes caused deposition of AApoAII amyloid fibrils in the tissues also may be favorable for AA amyloid fibrilization. These changes may be caused by certain factors, such as amyloid-enhancing factors (Kisilevsky, 1990; Shirahama et al., 1990), pathological chaperones, characteristics of HDL particle in which serum precursor of AA fibrils (apoSAA) circulates, or the presence of AApoAII fibrils with ß-pleated sheet structure which might enhance fibrilization of AA protein (Ganowiak et al., 1994).

Here we analyzed how one genotypic difference influences the degree and rate of progress of senescence in mice. The *Apoa2*^{c} gene, which was confirmed in this study to be responsible for the early onset of senile amyloidosis, shortens the life span of mice but does not change the rate of progress of senescence. What are the genetic factors responsible for the accelerated senescence of the SAMP1 strains? We are making genome maps of each SAM strain using mouse endogenous leukemia provirus and (CA) repeats (microsatellites) as genetic markers. Population analysis with congenic strains which have chromosomal regions found in common in the SAMP strains should provide some clues to an understanding of accelerated senescence.

ACKNOWLEDGMENTS

This work was supported in part by a grant from the Ministry of Health and Welfare of Japan. We are grateful to Dr. A. Ota of Kyoto University, Dr. K. Higuchi of Kyoto National Hospital, and D. Cary for helpful comments, and S. Yasuoka for technical assistance.

Address correspondence to Dr. Keiichi Higuchi, Department of Senescence Biology, Chest Disease Research Institute, Kyoto University, Sakyo-Ku, Kyoto 606, Japan.

REFERENCES

Benson, M.D. Inherited amyloidosis. J. Med. Genet. 28:73–78; 1991.

Chen, W.H.; Hosokawa, M.; Tsuboyama, T.; Ono, T.; Iizuka, T.; Takeda, T. Age related changes in the temporomandibular joint of the senescence accelerated mouse. Am. J. Pathol. 135:379–385; 1989.

Cohen, A.S.; Jones, L.A. Advances in amyloidosis. Curr. Opin. Rheumat. 5:62–76; 1993.

Coleman, D.L. Obese and diabetes: Two mutant genes causing diabetes-obesity syndromes in mice. Diabeteologia 14:41–48; 1978.

Finch, C.E. Longevity, senescence, and the genome. Chicago: The University of Chicago Press, 1990.

Ganowiak, K.; Hultman, P.; Engsrrom, U.; Gustavsson, A.; Westermark, P. Fibrils from systemic amyloid related peptides enhance development of experimental AA-amyloidosis in mice. Biochem. Biophys. Res. Commun. 199:306–312; 1994.

Gardner, M.B.; Ihle, J.N.; Pillarisetty, R.J.; Talal, N. Type C virus expression and host response in diet-cured NZB/W mice. Nature 268:341–344; 1977.

Gelman, R.; Watson, A.; Bronson, R.; Yunis, E. Murine chromosomal region correlated with longevity. Genetics 118:693–704; 1988.

Gompertz, B. On the nature of the function expressive of the law of human mortality, and on a new mode of determining the value of life contingencies. Philos. Trans. R. Soc. London 115:513–585; 1825.

Hang, L.; Theofilopoulos, A.N.; Dixon, F.J. A spontaneous rheumatoid arthritis-like disease in MRL/l mice. J. Exp. Med. 155:1690–1701; 1982.

Higuchi, K.; Matsumura, A.; Honma, A.; Takeshita, S.; Hashimoto, K.; Hosokawa, M.; Yasuhira, Y.; Takeda, T. Systemic senile amyloid in senescence accelerated mice: a unique fibril protein demonstrated in tissue from various organs by the unlabeled immunoperoxidase method. Lab. Invest. 48:231–240; 1983.

Higuchi, K.; Matsumura, A.; Honma, A.; Toda, T.; Takeshita, S.; Matsushita, M.; Yonezu, T.; Hosokawa, M.; Takeda, T. Age-related changes of serum apoprotein SAS_{SAM}, apoprotein A-I and low-density lipoprotein levels in Senescence-Accelerated Mouse (SAM). Mech. Ageing Dev. 26:311–326; 1984.

Higuchi, K.; Yonezu, T.; Kogishi, K.; Matsumura, A.; Takeshita, S.; Higuchi, K.; Kohno, A.; Matsushita, M.; Hosokawa, M.; Takeda, T. Purification and characterization of a senile amyloid-related antigenic substance ($apoSAS_{SAM}$) from mouse serum: $apoSAS_{SAM}$ is an apoA-II apolipoprotein of mouse high density lipoproteins. J. Biol. Chem. 261:12834–12840; 1986a.

Higuchi, K.; Takeda, T. Animal model. In: Marrink, J.; Van Rijiswijk, M.H., eds. Amyloidosis. Dordrecht, The Netherlands: Martinus Nijhoff, 1986b:283–290.

Higuchi, K.; Naiki, H.; Kitagawa, K.; Hosokawa, M.; Takeda, T. Mouse senile amyloidosis: AS_{SAM} amyloidosis in mice presents universally as a systemic age-associated amyloidosis. Virchows Arch. B: Cell Pathol. 60:231–239; 1991a.

Higuchi, K.; Kitagawa, K.; Naiki, H.; Hanada, K.; Hosokawa, M.; Takeda, T. Polymorphism of apolipoprotein A-II (apoA-II) among inbred strains of mice: relationship between the molecular type of apoA-II and mouse senile amyloidosis. Biochem. J. 279:427–433; 1991b.

Higuchi, K.; Kitado, H.; Kitagawa, K.; Kogishi, K.; Naiki, H.; Takeda, T. Development of congenic strains of mice carrying amyloidogenic apolipoprotein A-II (Apoa2^c): Apoa2^c reduces the plasma level and size of high density lipoprotein. FEBS Lett. 317:207–210; 1993.

Higuchi, K.; Naiki, H.; Kitagawa, K.; Kitado, H.; Kogishi, K.; Matsushita, T.; Takeda, T. Apolipoprotein A-II gene and development of amyloidosis and senescence in a congenic strain of mice carrying amyloidogenic apoA-II. Lab. Invest. 72:75–82; 1995.

HogenEsch, H.; Niewold, T.A.; Higuchi, K.; Tooten, P.C.J.; Gruys, E.; Radl, J. Gastrointestinal AApoAII and AA-amyloidosis in aged C57BL/Ka mice: amyloid-type dependent effect of long-term immunosuppressive treatment. Virchows Arch. B: Cell. Pathol. 64:37–43; 1993.

Holmgren, O.; Haettner, E.; Nordenson I.; Saudgren, O.; Steen, L.; Lundgren, E. Homozygosity for the transthyretin-met30-gene in two

Swedish sibs with familial amyloidotic polyneuropathy. Clin. Genet. 34:333–338; 1988.
Hosokawa, M. Grading score system: a method of evaluation of the degree senescence in senescence-accelerated mouse (SAM). In: Takeda, T., ed. The SAM model of senescence. Amsterdam: Excerpts Medica, 1994:23–28.
Hosokawa, M.; Kasai, R.; Higuchi, K.; Takeshita, S.; Shimizu, K.; Hamamoto, H.; Honma, A.; Irino, M.; Toda, K.; Matsumura, A.; Takeda, T. Grading score system: a method for evaluation of the degree of senescence in senescence accelerated mouse (SAM). Mech. Ageing Dev. 26:91–102; 1984.
Hosokawa, M.; Ashida, Y.; Nishikawa, T.; Takeda, T. Accelerated aging of dermal fibroblast-like cells from senescence-accelerated mouse (SAM). 1. Acceleration of population aging in vitro. Mech. Ageing Dev. 74:65–77; 1994.
Hosokawa, T.; Hosono, M.; Higuchi, K.; Aoike, A.; Kawai, K.; Takeda, T. Immune responses in newly developed short-lived SAM mice I: age-associated early decline in immune activities of cultured spleen cells. Immunology 62:419–423; 1987.
Ishikawa, S.; Higuchi, K.; Hosokawa, M.; Takeda, T. Marked decrease of apolipoprotein A-II and appearance of apoA-I-containing lipoprotein without apoA-II with advancing age in SAMP1. In: Takeda, T., ed. The SAM model of senescence. Amsterdam: Excerpta Medica, 1994:295–298.
Kaplan, E.L.; Meier, P. Nonparametric estimation from incomplete observation. J. Am. Stat. Assoc. 53:457–481; 1958.
Kisilevsky, R. Heparan sulfate proteoglycans in amyloidogenesis: an epiphenomenon, a unique factor, or the tip of more fundamental process? Lab. Invest. 63:589–591; 1990.
Kitado, H.; Higuchi, K.; Takeda, T. Molecular genetic characterization of the senescence-accelerated mouse (SAM) strains. J. Gerontol. Biol. Sci. 49:B247–B254; 1994.
Kitagawa, K.; Naiki, H.; Takeda, T.; Higuchi, K. Age-associated decrease in the mRNA levels and the rate of synthesis of apoA-II in murine senile amyloidosis. Lab. Invest. 70:565–571; 1994.
Kohno, A.; Yonezu, T.; Matsushita, M.; Irino, M.; Higuchi, K.; Higuchi, K.; Takeshita, S.; Hosokawa, M.; Takeda, T. Chronic food restriction modulates the advance of senescence in the senescence accelerated mouse (SAM). J. Nutr. 115:1259–1266; 1985.
Kurozumi, M.; Matsushita, T.; Hosokawa, M.; Takeda, T. Age-related changes in lung structure and function in the senescence-accelerated mouse (SAM): SAM-P/1 as a new murine model of senile hyperinflation of lung. Am. J. Respir. Crit. Care Med. 149:776–782; 1994.
Lane, P.W.; Dickie, M.M. The effect of restricted food intake on the life span of genetically obese mice. J. Nutr. 64:549–554; 1958.
Lorenzo, A.; Razzaboni, B.; Weir, G.C.; Yankner, B.A. Pancreatic islet cell toxicity of amylin associated with type-2 diabetes mellitus. Nature 368:756–760; 1994.
Makino, S.; Kunimoto K.; Nuraoka, Y.; Mizushima, Y.; Katagiri, K.; Tochino, Y. Breeding of a non-obese diabetic strain of mice. Exp. Anim. 291:1–13; 1980.
Martin, G.M. Genetic syndromes in man with potential relevance to the pathobiology of aging. In: Bergsma, D.; Harrison, D.E., eds. Genetic effects on aging. Birth defects. [Orig. Artic. Ser. 14]. New York: Liss, 1978:5–39.
Matsumura, A.; Higuchi, K.; Shimzu, K.; Hosokawa, M.; Hashimoto, K.; Yasuhira, K.; Takeda, T. A novel amyloid fibril protein isolated from senescence-accelerated mice. Lab. Invest. 47:270–275; 1982.
Matsushita, M.; Tsuboyama, T.; Kasai, R.; Okumura, H.; Yamamuro, T.; Higuchi, K.; Kohno, A.; Yonezu, T.; Utani, A.; Umezawa, M.; Takeda, T. Senescence-accelerated mouse (SAM): SAM-R/3 and SAM-P/6 as a new murine model for senile osteoporosis. Am. J. Pathol. 125:276–283; 1986.
Maury, C.P.J. Molecular pathogenesis of ß-amyloidosis in Alzheimer's disease and other cerebral amyloidoses. Lab. Invest. 72:4–16; 1995.
Mehrabian, M.; Qiao, J-H.; Hyman, R.; Ruddle, D.; Laughton, C.; Lusis, A.J. Influence of the apoA-II gene locus on HDL levels and fatty streak development in mice. Arterioscler. Thromb. 13:1–10; 1992.
Naiki, H.; Higuchi, K.; Nakakuki, K.; Takeda, T. Kinetic analysis of amyloid fibril polymerization in vitro. Lab. Invest. 65:104–110; 1991.
Naiki, H.; Higuchi, K.; Shimada, A.; Takeda, T.; Nakakuki, K. Genetic analysis of murine senile amyloidosis. Lab. Invest. 68:332–337; 1993.
Nisitani, S.; Hosokawa, M.; Sasaki, M.S.; Yasuoka, K.; Naiki, H.; Mastushita, T.; Takeda, T. Acceleration of chromosome aberrations in senescence-accelerated strains of mice. Mutat. Res. 237:221–228; 1990.
Paigen, B.; Mitchell, D.; Reue, K.; Morrow, A.; Lusis, A.J.; LeBoeuf, R.C. Ath-1, a gene determining atherosclerosis susceptibility and high density lipoprotein levels in mice. Proc. Natl. Acad. Sci. USA 84:3763–3767; 1987.
Saitoh, Y.; Hosokawa, M.; Shimada, A.; Watanabe, Y.; Yasuda, T.; Nagawa, Y.; Takeda, T. Age-related hearing impairment in senescence-accelerated mouse (SAM). Hearing Res. 75:27–37; 1994.
Shimada, A.; Ohta, A.; Akiguchi, I.; Takeda, T. Inbred SAM-P/10 as a model of spontaneous, inherited brain atrophy. J. Neuropathol. Exp. Neurol. 51:440–450; 1992.
Shimada, A.; Hosokawa, M.; Ohta, A.; Akiguchi, I.; Takeda, T. Localization of atrophy-prone areas in the aging mouse brain: comparison between the brain atrophy model SAM-P/10 and the normal control SAM-R/1. Neuroscience 59:859–869; 1994.
Shimizu, K.; Morita, H.; Niwa, T.; Maeda, K.; Shibata, M.; Higuchi, K.; Takeda, T. Spontaneous amyloidosis in senile NSY mice. Acta Pathol. Jpn. 43:215–221; 1993.
Shirahama, T.; Miura, K.; Ju, S.T.; Kisilevsky, R.; Gruys, E.; Cohen, A.S. Amyloid enhancing factor-loaded macrophages in amyloid fibril formation. Lab. Invest. 62:61–68; 1990.
Steel, R.G.D.; Torrie, J.H. Principles and procedures of statistics; a biometrical approach. New York: McGraw Hill, 1980.
Storer, J. Effect of aging and radiation in mice of different genotypes. In: Harrison, D.E., ed. Genetic effects on aging. New York: Liss, 1978:55–71.
Takeda, T.; Hosokawa, M.; Takeshita, S.; Irino, M.; Higuchi, K.; Matsushita, T.; Tomita, Y.; Yasuhira, K.; Hamamoto, H.; Shimizu, K.; Ishii, M.; Yamamuro, T. A new murine model of accelerated senescence. Mech. Ageing Dev. 17:183–194; 1981.
Takeda, T.; Hosokawa, M.; Higuchi, K. Senescence-accelerated mouse (SAM): a novel murine model of accelerated senescence. J. Am. Geriatr. Soc. 39:911–919; 1991.
Takeda, T.; Hosokawa, M.; Higuchi, K. Senescence-accelerated mouse (SAM): a novel murine model of aging. In: Takeda, T., ed. The SAM model of senescence. Amsterdam: Excerpta Medica, 1994:15–22.
Takeshita, S.; Hosokawa, M.; Irino, M.; Higuchi, K.; Shimizu, K.; Yasuhira, K.; Takeda, T. Spontaneous age-associated amyloidosis in senescence-accelerated mouse (SAM). Mech. Ageing Dev. 20:13–23; 1982.
Umezawa, M.; Hosokawa, M.; Kohno, A.; Ishikawa, S.; Kitagawa, K.; Takeda, T. Dietary soybean protein compared with casein retards senescence in the senescence-accelerated mouse. J. Nutr. 123:1905–1912; 1993.
Warden, C.H.; Hedrick, C.C.; Qiao. J.-H.; Castellani, L.W.; Lusis, A.J. Atherosclerosis in transgenic mice over expressing apolipoprotein A-II. Science 261:469–472; 1993.
Yagi, H.; Irino, M.; Matsushita, T.; Katoh, S.; Umezawa, M.; Tsuboyama, T.; Hosokawa, M.; Akiguchi, I.; Tokunaga, R.; Takeda, T. Spontaneous spongiform degeneration of brain stem in SAM-P/8 mice, a newly developed memory-deficient strain. J. Neuropathol. Exp. Neurol. 48:577–590; 1989.
Yonezu, T.; Higuchi, K.; Tsunasawa, S.; Takagi, S.; Sakiyama, F.; Takeda, T. High homology is present in the primary structures between murine senile amyloid protein (AS_{SAM}) and human apolipoprotein A-II. FEBS Lett. 203:149–152; 1986.
Yoshinaga, T.; Nakazato, M.; Ikeda, S.; Ohnishi, A. Homozygosity for the transthyretin-met30 gene in three siblings with type I familial amyloidotic polyneuropathy. Neurology 42:2045–2047; 1992.
Zang, S.H.; Reddick, R.L.; Priedrahita, J.A.; Maeda, N. Spontaneous hypercholesterolemia and arterial lesions in mice lacking apolipoprotein E. Science 258:468–471; 1992.
Zhao, X.-H.; Nomura, Y. Age-related changes in uptake and release on L-[^{3}H]noradrenaline in brain slices of senescence-accelerated mouse. Int. J. Dev. Neurosci. 8:267–272; 1990

Received April 25, 1995
Accepted October 3, 1995